Magnetic Resonance in Medicine 56:1371–1374 (2006)

Presentation of 3D Isotropic Imaging Data for Optimal Viewing

R. Mark Henkelman,* Leila Baghdadi, and John G. Sled

Three-dimensional (3D) isotropically sampled data facilitates retrospective viewing of arbitrarily aligned image planes and simplifies automated computer analysis of 3D structures. However, compared to acquisitions that employ thick slices, MRI acquisitions with isotropic sampling have a lower signal-to-noise ratio (SNR). A rater study was performed to examine viewer preference for the trade-off between SNR and the partial-volume effect of through-plane averaging. A robust preference for a 5:1 ratio in through-plane to in-plane was found for a typical SNR of 11. Magn Reson Med 56:1371–1374, 2006.

Key words: 3D isotropic imaging; viewer preference; asymmetric voxels; signal-to-noise ratio

Since spatial localization is performed electronically in magnetic resonance imaging (MRI), this method provides remarkable flexibility in the choice of the data to be acquired. Acquisition planes can be along the three dominant axes or at arbitrary oblique angles, voxels can be of arbitrary size in any direction, and fields of view (FOVs) can be made to fit the object. This flexibility can be used to considerable advantage when tailored for specific applications or anticipated outcomes.

When imaging a broad range of structures that may be subsequently viewed in arbitrary orientations, isotropic data acquisition is the only unbiased option. In contrast, when predetermined orientations of viewing are chosen perpendicular to the dominant orientation of the structure, it is customary to acquire slices with voxel dimensions through the slice that are significantly larger than voxel dimensions within the slice. There are two reasons for this choice: 1) the larger voxel dimension through the slice provides a greater signal-to-noise ratio (SNR) while high resolution is maintained within the slice, and 2) slice-select gradients frequently are not strong enough to achieve through-slice resolution, which is equivalent to in-plane resolution, particularly when fast data acquisitions are required. Voxel asymmetries are typically 5:1 (through-slice voxel dimension to in-slice dimension), although extreme examples of 20:1 are encountered in the literature (1–5). Such extreme voxels are often inadvertently acquired without recognizing that partial-volume effects through the slice degrade the effective resolution.

Mouse Imaging Centre, Hospital for Sick Children, Toronto, Ontario, Canada.
Grant sponsor: Ontario Research and Development Challenge Fund.
*Correspondence to: R. Mark Henkelman, Ph.D., Director, Mouse Imaging Centre, Hospital for Sick Children, 555 University Ave., Toronto, Ontario M5G 1X8, Canada. E-mail: mhenkel@phenogenomics.ca
Received 13 June 2006; revised 27 July 2006; accepted 9 August 2006.
DOI 10.1002/mrm.21077
Published online 30 October 2006 in Wiley InterScience (www.interscience.wiley.com).

The purpose of this article is to examine whether 3D isotropic data should be displayed with through-plane averaging to achieve better visual SNR.

MATERIALS AND METHODS

Three-dimensional (3D) isotropic images of a fixed mouse brain retained in its skull (6) were acquired on a 7 T Varian INOVA scanner using a fast spin-echo (FSE) pulse sequence (TR/TE = 325/8 ms) with six echoes (with the center of *k*-space acquired on the fourth echo, TE_{eff} = 32 ms), FOV = 12 mm × 12 mm × 25 mm, acquisition matrix of 432 × 432 × 780, and four signal averages. A variable gain acquisition was used to accommodate the large dynamic range of the 3D acquisition (7). The total imaging time was 11.2 hr, and an image with 32 μm isotropic voxels was obtained. The acquisition parameters were specified to facilitate computer registration, segmentation, and statistical analysis to detect differences in neuroanatomy caused by mutations in otherwise genetically identical groups of mice (8,9). Thus, there was no a priori task that would determine an optimal slice direction for multislice imaging. The basic SNR of these acquired data was 26. When data of lower SNR were required, additional noise was simulated with a Gaussian random number generator. In general, adding Gaussian noise to a magnitude image is not procedurally correct since it can yield negative pixels. However, in the case of high-SNR images (>5), it is an acceptable approximation (10). The first experiment was performed with an SNR of 11.

A representative horizontal slice through the brain was chosen, which showed highly detailed structures as well as extended structures that were distinguishable but with minimal contrast. A set of test images was generated with increasing amounts of averaging through the chosen slice consisting of 1, 3, 5, 7, 9, 11, and 13 pixels. Signal intensity was renormalized by dividing the summed image by the number of pixels added. The isotropic image with SNR = 11 is shown in Fig. 1 along with subpanels from the through-plane average set.

Two additional comparison choices were generated to determine whether the optimum viewer preference was simply a function of image SNR or the through-plane averaging was intrinsically beneficial. To this end, the 3- and 5-pixel through-plane averaging images were compared with a single-pixel-thickness image that was smoothed using an in-plane cylindrical Gaussian filter over the adjacent eight points to produce an SNR that in theory was equivalent to the SNR of the through-plane images. An example set is shown in Fig. 2.

This set of test images was presented to 12 experienced MR readers. The readers were asked to pick the images in which they could best see the neuroanatomy. For the set of

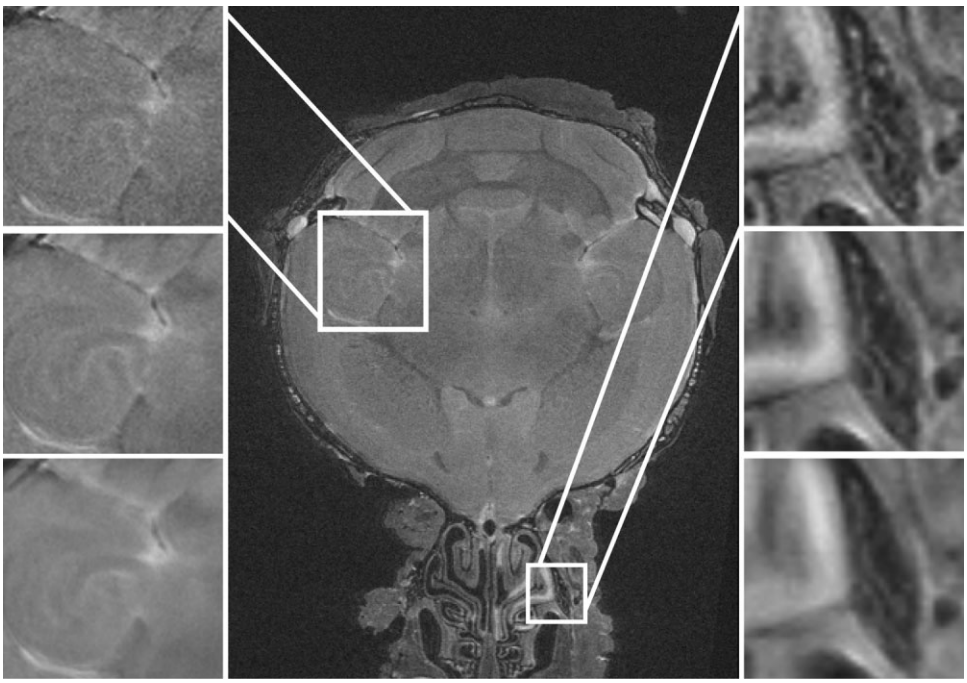

FIG. 1. Illustration of the effect of through-plane averaging on the appearance of 3D isotropic data. The central panel shows a representative slice from a mouse brain data set taken at 32-μm isotropic resolution. The images on the left show an enlargement of a region of relatively homogenous signal intensity with low contrast variations. The column of image on the right shows data with high-definition detail. From top to bottom, the side bar images are a single-pixel average at the top, five pixels in the middle, and 13 averages in the lower panel.

through-plane filters, images were presented three at a time in random order and the viewers were asked to reject the least-informative image, which was then replaced with another image until only three were left. At this point the viewers were requested to rank order the three remaining images from best to worst in terms of their ability to see neuroanatomical content. The best image was given a score of 1; second best, a score of ½; and third best, a score of ¼. During the tests the viewers were able to change the window, level, and magnification zoom, and to pan over the images either independently or locked in synchrony. This gave the viewers complete flexibility to view the images in a presentation that was most comfortable and familiar to them.

Following the through-plane series, the viewers were asked to compare the pair of images with approximately equivalent SNRs. The viewers were asked simply to choose which of the two images best showed the anatomy. Reader reproducibility was retested by repeating the reading 3 weeks later. Two additional 3D isotropic data sets of the same resolution were generated with SNRs of 26 and 5. The complete study was repeated using each of these new data sets with higher and lower SNRs.

RESULTS

Figure 3 shows the measured standard deviation (SD) of signal intensity over a large region of the presented image, for each of the test images used in the study. The horizontal axis calculates the expected relative root mean squared deviation (RMSD) noise that would be measured if the images had homogeneous intensity over the whole volume

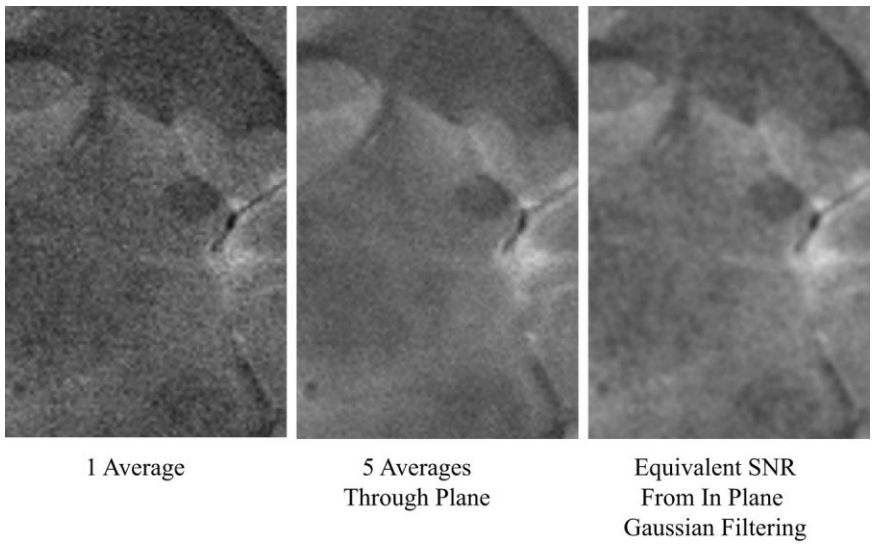

FIG. 2. Another region taken from the central image in Fig. 1, showing a single average on the left, with five averages through the plane in the middle, and on the right an equivalent SNR obtained by Gaussian filtration within the 32-μm plane. The in-plane averages were always less acceptable than the through-plane averaging.

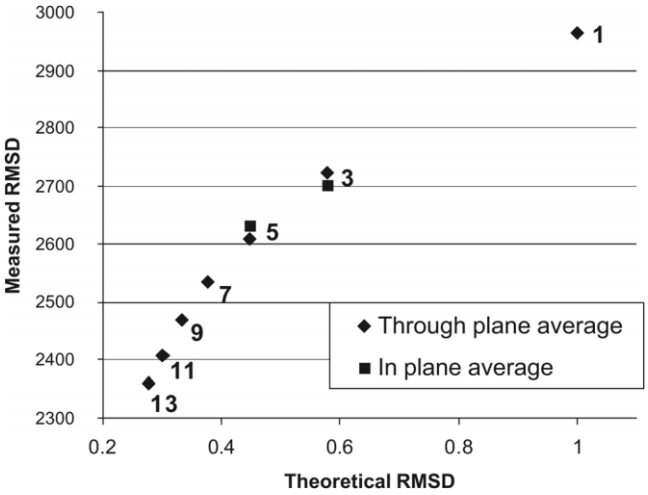

FIG. 3. This figure shows a measured RMSD in an ROI within the image for various filtering regimes. This is plotted against the theoretical RMSD that would be obtained if the image had uniform intensity with purely uncorrelated Gaussian noise. There is a strong correlation between the two evaluations of noise. The measured RMSD is considerably larger because of structural anatomical variation within the image, and falls more rapidly because both the anatomical structure and the noise are attenuated as more slices are averaged. The square symbols show measured noise in images that were filtered with Gaussian in-plane filters only and were designed to match the three-and fivefold through-plane averaging.

with an additive random uncorrelated Gaussian noise. On the basis of this simple model, noise would be expected to be proportional to $1/\sqrt{n}$, where n is the number of through-plane pixels averaged. The measured noise has a similar structure but is significantly offset by the contribution of anatomical variability to the measured SD. The actual measured noise falls faster than the expected noise since the correlated but varying structure through the slice is also averaged out with through-plane averaging. The test images with equivalent SNR produced by in-plane Gaussian filtration have noise that is within 2% of their comparable through-plane averages. The slight variance from the expected value is again due to the effective averaging of biological structure by these filters.

Figure 4a shows a histogram of the weighted reader preference over all 12 readers when different amounts of through-plane averaging are compared for an original image SNR of 11. Partial weightings for second and third choices were introduced because the ordering of the first and second choices was sometimes reversed on the test/retest measurements, suggesting that the second and third choices were partially informative. The preference for through-slice averaging is five slices (median) and an interquartile range of 3–7.

In the case of in-plane averaging, in neither of the two comparisons did any of the 12 reviewers prefer the image that had achieved improved SNR through in-plane averaging.

Thus, there was a high degree of concordance among all 12 viewers in terms of preference. On the retest experiment repeated 3 weeks later, the observers' first-choice preferences were identical 82% of the time. The high degree of agreement rendered sophisticated statistical metrics unnecessary.

For the higher-SNR data set (SNR = 26), all observers still rejected in-plane smoothing but were less inclined to adopt through-plane averaging. The results are shown in Fig. 4b. Here the preferred median number of through-plane pixels averaged is 3, with an interquartile range of 1–3. For data with a very low original SNR of 5, viewers preferred more through-slice averaging, as shown in Fig. 4c, with a median of 7 and an interquartile range of 5–11.

DISCUSSION

For viewing 3D isotropic data with an intermediate SNR of 11, the viewers preferred fivefold through-plane averaging for optimal visualization of anatomy averaging. Greater than 7-pixel through-plane averaging gave better SNR but decreased visibility of small structures due to partial-volume averaging. On the other hand, less than fivefold through-plane averaging yielded higher contrast of smaller detailed structures, but with a lower SNR.

In no case did viewers prefer images that had improved SNR arising from in-plane averaging. Such images were always described as "too blurry." This can be understood intuitively because one can approximate in-plane averaging visually by squinting or viewing the image from a distance. Thus, numerical in-plane averaging can add no real advantage to the visual observer. On the other hand, through-plane averaging introduces new data with uncorrelated noise that cannot be replicated in any way by varying the manner of visual observation. Thus it is not surprising that SNR gains obtained by through-plane averaging are always preferred to the same SNR gain achieved by averaging within the plane.

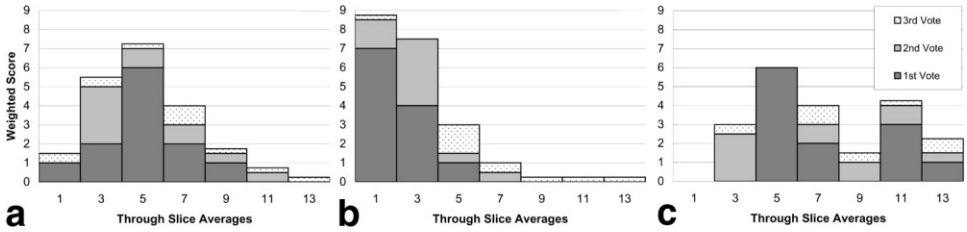

FIG. 4. The distribution of preferred image filters as determined by 12 individuals. Each individual gave a first, second, and third vote. The first votes were counted as a unit weight, second votes as a half weight, and third votes as a quarter weight. **a:** The preference for through-slice averaging was for five slices (in this case, when the original SNR of the isotropic data was 11). **b:** Preferences with original SNR = 26. **c:** Preferences with original SNR = 5.

It is interesting to note that the results of this study correspond closely to the "rule of thumb" for multislice imaging, which holds that the slice thickness should be approximately five times the in-plane resolution. This "rule of thumb" comes from informal observer optimization over many years of clinical practice. As is often the case, the cumulative experience of clinical radiologists is an effective and alternative optimization strategy.

It is worth noting that the usual method of measuring relative SNR (i.e., by measuring intensity in a region of the image and the SD or mean of a clear and unartifacted background region) could not be used in this study. This is because the background noise in the original magnitude image is Rayleigh distributed (11,12). When several Rayleigh distributions are averaged, the resulting distribution is no longer Rayleigh in shape, and the distribution becomes narrower as more through-plane voxels are included. Although the SD of these background distributions falls by 2.6-fold in going from one to 13 averages, the mean of the background intensity actually increases by 1%. This cautionary note is not of significance to the present study, and one could ameliorate the anomalous background noise behavior by filtering prior to computing the magnitude of the complex image data.

It should also be pointed out that this SNR recovery by through-plane averaging is not as efficient as planning for acquiring thicker slices when the preferred direction of viewing is clear from the outset. A fivefold averaging through-plane improves the SNR by $\sqrt{5}$ (= 2.24) times, but requires a fivefold longer imaging time. However, if it is determined a priori that multislice imaging with asymmetric voxels is appropriate for viewing, the longer imaging time could be used to acquire five signal averages, which would also yield an SNR gain of $\sqrt{5}$. Thus, for equivalent acquisition times, multislice imaging with asymmetric voxels is five times more advantageous than 3D isotropic imaging with through-plane averaging.

Finally, if 3D isotropic data are to be viewed with a predefined visual SNR of SNR_0 and a resolution of r, this method allows for data to be obtained at a resolution of $r \times 5^{-1/6} = 0.765r$ and with an associated reduced SNR = $SNR_0 / \sqrt{5} = 0.447\ SNR_0$. The required visual SNR_0 can then be recovered by through-plane averaging in the display. Thus, the in-plane resolution can be reduced by 23% while maintaining the visual SNR if through-plane averaging of five pixels is used.

Since through-plane averaging can be implemented rapidly on any image visualization program, software can be written to execute this operation for arbitrary rectilinear and oblique viewing planes as a standard display feature. For oblique viewing, the through-plane voxels will not be in a regular column, which will necessitate sinc interpolation in adjacent planes. Such an algorithm can be built into the viewing software in a way that is transparent to the observer.

CONCLUSIONS

Isotropic 3D image data acquired for arbitrary viewing or for computer analysis can be displayed for better visibility if through-plane data are averaged over a thickness of 3–7 voxels, depending on the SNR of the original data.

ACKNOWLEDGMENTS

This work was conducted at the Mouse Imaging Centre at the Hospital for Sick Children and the University of Toronto. The infrastructure was funded by the Canada Foundation for Innovation and Ontario Innovation Trust. The research was funded by an Ontario Research and Development Challenge Fund grant to the Ontario Consortium for Small Animal Imaging. R. Mark Henkelman holds a Canada Research Chair in Imaging.

REFERENCES

1. Jung B, Zaitsev M, Hennig J, Markl M. Navigator gated high temporal resolution tissue phase mapping of myocardial motion. Magn Reson Med 2006;55:937–942.
2. Szarf G, Dori Y, Rettmann D, Tekes A, Nasir K, Amado L, Foo TKF, Bluemke DA. Zero filled partial Fourier phase contrast MR imaging: in vitro and in vivo assessment. J Magn Reson Imaging 2005;23:42–49.
3. Hsu L-Y, Ingkanisorn WP, Kellman P, Aletras AH, Arai AE. Quantitative myocardial infarction on delayed enhancement MRI. Part II: clinical application of an automated feature analysis and combined thresholding infarct sizing algorithm. J Magn Reson Imaging 2006;23:309–314.
4. Mohajer K, Zhang H, Gurell D, Ersoy H, Ho B, Kent KC, Prince MR. Superficial femoral artery occlusive disease severity correlates with MR cine phase-contrast flow measurements. J Magn Reson Imaging 2006; 23:355–360.
5. Regatte RR, Akella SVS, Lonner JH, Kneeland JB, Reddy R. $T_{1\rho}$ relaxation mapping in human osteoarthritis (OA) cartilage: comparison of $T_{1\rho}$ with T_2. J Magn Reson Imaging 2006;23:547–553.
6. Henkelman RM, Dazai J, Lifshitz N, Nieman BJ, Tsatskis S, Lerch J, Bishop J, Kale S, Sled JG, Chen XJ. High throughput microimaging of the mouse brain. In: Proceedings of the 14th Annual Meeting of ISMRM, Seattle, WA, USA, 2006. p 2010.
7. Behin R, Bishop J, Henkelman RM. Dynamic range requirements for MRI. Concepts Magn Reson B (Magn Reson Eng) 2005;26B:28–35.
8. Lerch J, Tsatskis S, Sled JG, Kovacevic N, Henkelman RM. Variability of automated shape analyses of fixed brain mouse MRI. In: Proceedings of the 14th Annual Meeting of ISMRM, Seattle, WA, USA, 2006. p 1504.
9. Tsatskis S, Lerch J, Carroll J, Hayden MR, Henkelman RM. High-resolution 3D MRI to identify neurodegeneration in a Huntington disease mouse model brain. In: Proceedings of the 14th Annual Meeting of ISMRM, Seattle, WA, USA, 2006. p 3392.
10. Bernstein MA, Thomasson DM, Perman WH. Improved detectability in low signal-to-noise ratio magnetic resonance images by means of a phase-corrected real reconstruction. Med Phys 1989;16:813–817.
11. Henkelman RM. Measurement of signal intensities in the presence of noise in MR images. Med Phys 1985;12:232–233.
12. Henkelman RM. Erratum. Med Phys 1986;13:544.